



HAL
open science

Nanocasting of fibrous morphology on a substrate for long-term propagation of human induced pluripotent stem cells

Sisi Li, Momoko Yoshioka, Junjun Li, Li Liu, Shixin Ye, Ken-Ichiro Kamei, Yong Chen

► **To cite this version:**

Sisi Li, Momoko Yoshioka, Junjun Li, Li Liu, Shixin Ye, et al.. Nanocasting of fibrous morphology on a substrate for long-term propagation of human induced pluripotent stem cells. *Biomedical Materials*, 2022, 17 (2), pp.025014. 10.1088/1748-605X/ac51b8 . hal-03601217

HAL Id: hal-03601217

<https://hal.science/hal-03601217>

Submitted on 8 Mar 2022

HAL is a multi-disciplinary open access archive for the deposit and dissemination of scientific research documents, whether they are published or not. The documents may come from teaching and research institutions in France or abroad, or from public or private research centers.

L'archive ouverte pluridisciplinaire **HAL**, est destinée au dépôt et à la diffusion de documents scientifiques de niveau recherche, publiés ou non, émanant des établissements d'enseignement et de recherche français ou étrangers, des laboratoires publics ou privés.

Nanocasting of fibrous morphology on a substrate for long-term propagation of human induced pluripotent stem cells

Sisi Li^{a,b}, Momoko Yoshioka^a, Junjun Li^a, Li Liu^a, Shixin Ye^c, Ken-ichiro Kamei^a, Yong Chen^{a,b}*

^a Institute for Integrated Cell-Material Science, Kyoto University, Kyoto 606-8501, Japan

^b Ecole Normale Supérieure, CNRS-ENS-UPMC UMR 8640, 24 rue Lhomond, 75005 Paris, France

^c U1195, Institut National de la Santé et de la Recherche Médicale (INSERM), University of Paris-Saclay, 94276 Le Kremlin Bicêtre, France

Abstract:

Human-induced pluripotent stem cells (hiPSCs) can be self-renewed for many generations on nanofibrous substrates. Herein, a casting method is developed to replicate the nanofibrous morphology into a thin layer of polymethylsiloxane (PDMS). The template is obtained by electrospinning and chemical crosslinking of gelatin nanofibers on a glass slide. The replicas of the template are surface-functionalized by gelatin and used for propagation of hiPSCs over tenth generations. The performance of the propagated hiPSCs is checked by immunofluorescence imaging, flowcytometry, and RT-PCR, confirming the utility of the method. The results are also compared with those obtained using electrospun nanofiber substrates. Inherently, the PDMS replicas is of low stiffness and can be reproduced easily. Compared to other patterning techniques, casting is more flexible and cost-effective, suggesting that this method might find applications in cell-based assays that rely on stringent consideration of both substrate stiffness and surface morphology.

Keywords: Nanocasting; Nanofiber; Substrate; Extracellular matrix; Stem cells

1. Introduction

Human-induced pluripotent stem cells (hiPSCs) are now widely used for disease modeling, drug testing, and regenerative medicine [1-5], due to their ability to self-renew and differentiate into multiple cell lineages. Indeed, a large number of protocols were proposed for lineage-specific differentiations [6, 7] and organoid generation [8]. Particular attention has to be paid, however, to the culture conditions in order to achieve high quality hiPSC products. In the case of hiPSC renewing, for example, feeder cells were initially used [1] but feeder-free and serum-free culture was found more suitable by using substrates coated with extracellular matrix (ECM) proteins [9]. Matrigel, an ECM mixture secreted by Engelbreth-Holm-Swarm (EHS) mouse sarcoma cells, is often used as coating agent which is convenient but contains unknown animal factors [10]. Other coating agents such as recombinant laminin [11, 12], recombinant vitronectin [13], and synthetic peptides [14, 15] can also be used for multiple passages. In both cases, the cost is an issue and it is desirable to find alternative ways by considering, for example, substrates with appropriate surface morphologies.

Human-induced pluripotent stem cells (hiPSCs) are now widely used for disease modeling, drug testing, and regenerative medicine [1-5], due to their ability to self-renew and differentiate into multiple cell lineages. Indeed, a large number of protocols were proposed for lineage-specific differentiation [6, 7] and organoid generation [8]. Particular attention has to be paid, however, to the culture conditions in order to achieve high-quality hiPSC products. In the case of hiPSC renewing, for example, feeder cells were initially used [1] but feeder-free and serum-free culture was found more suitable by using substrates coated with extracellular matrix (ECM) proteins [9]. Matrigel, an ECM mixture secreted by Engelbreth-Holm-Swarm (EHS) mouse sarcoma cells, is often used as a coating agent which is convenient but contains unknown animal factors [10]. Other coating agents such as recombinant laminin [11, 12], recombinant vitronectin [13], and synthetic peptides [14, 15] can also be used for multiple passages. In both cases, the cost is an issue and it is desirable to find alternative ways by considering, for example, substrates with appropriate surface morphologies.

Previously, we have shown that long-term expansion of hiPSCs could be achieved by using gelatin nanofiber-covered substrates produced by electrospinning and chemical crosslinking [16]. Propagation of hiPSCs over more than 20 passages has been demonstrated without introducing

any abnormal chromosome. Moreover, the passage of the cells could be done without enzymatic disassociation nor mechanic cutting, thus allowing a better hiPSC expansion. This is because the fact that gelatin is rich in arginine-glycine-aspartate (RGD) peptide sequences and that the nanofibrous morphology is in favor of cell adhesion and signaling pathway activation [17]. Moreover, gelatin is widely used in cosmetic, food, and medical industries and can be easily processed. However, previous studies have shown that hiPSCs cannot propagate on flat gelatin layers, due to insufficient cell attachment and rapid loss of pluripotency after a few passages [16, 18]. This would suggest that hiPSCs are very sensitive to the surface morphology of the gelatin substrate and that the nanofibrous pattern would allow more efficient cell anchoring on the substrate and pluripotency maintenance of the cells [16]. Generally speaking, the properties of the substrate, including its stiffness, permeability, morphology, and chemical composition, influence to a large extent the behavior of the cells such as adhesion, proliferation, survival, and differentiation [19-27]. Intuitively, the nanofibrous morphology resembles some parts of in vivo ECMs, which provides more appropriate ligand accessibility and spaces underneath of the cells for diffusional transport of cytokines and large proteins [16,29-32].

Electrospinning is a versatile and low-cost technique that works with different types of materials or material compositions [28-37]. However, this technique lacks repeatability and reproducibility when applied to collagen nanofiber deposition. Critical control of the environment temperature and humidity is even requested for electrospinning of high-quality gelatin nanofibers [16]. Herein, we develop a simple and low-cost technique, nanocasting, to reproduce a nanofibrous surface morphology from a substrate (template) defined by electrospinning. Since a template can be used many times in nanocasting, the replicas obtained with the same template may have the same fibrous morphology (positive or negative tones). This would allow us to overcome the lack of reproducibility of electrospun nanofibers. Nanocasting is now widely used to cast polydimethylsiloxane (PDMS) with a template. Previously, we have created artificial lotus leave by casting PDMS with a natural lotus, showing a high fidelity of replication [38]. Nevertheless, most of the templates were produced by electron beam lithography and reactive ion etching techniques [39, 40] and natural templates were often used to study the superhydrophobicity of plates or inserts [38, 41]. In this work, the template is simply produced by electrospinning and chemical crosslinking techniques, and both negative tone (PDMS replica) and positive tone (PDMS replica²) replicas were produced in order to compare their performance in long-term

hiPSCs propagation, using the nanofiber-covered substrate as control. We will show that the PDMS replica is able to support hiPSC propagation over the tenth generation whereas the PDMS replica² leads to spontaneous differentiation of the hiPSCs after a few passages.

2. Material and methods

2.1 Template fabrication

The template was fabricated by electrospinning and chemical crossing of gelatin nanofibers [16]. Briefly, 10 wt% gelatin powder from porcine skin (G2625, Sigma-Aldrich, France) was dissolved in a solution of acetic acid, ethyl acetate (Sigma-Aldrich, France), and de-ionized (DI) water with the volume ratio of 21:14:10. The solution was loaded into a syringe which is mounted in a syringe pump (KD Scientific). The needle of the syringe which served as spinneret was connected to the anode of a high potential power supply (TechDempaz, Japan) with a bias voltage of 11 KV and a silicon wafer placed 12 cm far away from the spinneret is grounded on which a cover glass (25 mm diameter; Matsunami Glass Ind., Ltd, Japan) was taped for the nanofiber connection. The flow rate of the gelatin solution was fixed at 0.2 ml/h. After electrospinning, gelatin nanofibers were dried in a 37°C vacuum overnight and cross-linked in a 0.2 M mixture of 1-ethyl-3-(3- dimethyl aminopropyl) carbodiimide hydrochloride (EDC; Dojindo, Japan) and N-hydroxysuccinimide (NHS; Sigma-Aldrich, Japan) in ethanol for 4 h. After crosslinking, samples were rinsed with 99.5% ethanol twice and dried in a vacuum at 37°C overnight. The sample fabrication process was used for the fabrication of the culture substrates of the control.

2.2 Nanocasting and surface coating of the replicas

Firstly, the template was fixed in a petri-dish with adhesion tapes. A prepolymer solution of PDMS at a ratio of 10:1 was poured on the template at 1 mm thickness. After removing air bubbles in a desiccator, the PDMS layer was cured for 2 h in an 80 °C oven, peeled-off from the template, and bonded on a glass slide after surface treating in air plasma. When this 1st (negative tone) replica was used as a template for the casting of a 2nd replica, the surface of PDMS was treated in a vapor of trimethylchlorosilane (TMCS) to facilitate the template separation. Then, it was used to produce the 2nd (positive tone) replica using the same casting parameter.

Before being used for hiPSC propagation, the replica (negative and positive) was spin-coated with 0.1 wt% gelatin dissolved in the mixed solution of acetic acid, ethyl acetate, and DI water at

a volume ratio of 21:14:10. Before spin-coating, the replica was treated with plasma for 3 min and the gelatin solution was deposited with as spin-coater at 3000 rpm for 60 s. After drying in a 37°C vacuum overnight, it was crosslinked using the same method as gelatin nanofibers. Afterward, the PDMS replicas were used for hiPSCs culture.

2.3 hiPSC expansion

253G1 hiPSCs from Kyoto University (CiRA) have been used in this work. Before cell loading, the substrate was rinsed with 99.5% ethanol 3 times for sterilization. Dissociated hiPSCs harvested from gelatin nanofiber substrate were introduced on a PDMS replica or replica² at a density of about 4×10^4 cells/cm² with a widely-used hiPSC culture medium mTeSR1 (Stem Cell Technologies) [42], supplemented with 10 μ M ROCK inhibitor (Y-27632; Wako Chemicals, Japan) [43]. The cells were cultured in the 37 °C incubator with 5% CO₂ (IP400 CO₂ incubator). The medium was changed every day. After 48 h, the ROCK inhibitor was removed. When cells reached 80% of confluency on day 4, they were treated with a cell dissociated no-enzyme solution (GIBCO) for 5 min at 37 °C. Cells were then dissociated by hand pipetting over 10 times to a single cell level and transferred onto a new PDMS replica or replica². Similarly, gelatin nanofiber substrate was used as a control.

2.4 Characterization

Atomic Force Microscope (AFM) imaging: Nanofibrous morphology of template and replica were analyzed using an atomic force microscope (Agilent 5500 AFM) in tapping mode with SPM probes (AppNano).

Contact angle measurement: The contact angle measurement has been done by using the sessile drop method. A 2 μ l water droplet was deposited onto the sample, and the water/substrate interface was captured by a CCD camera. The edge of the droplet was then analyzed using a sessile drop-fitting model.

Immunocytochemistry: Cells were firstly fixed in 4% paraformaldehyde at room temperature for 30 min; permeabilized with 0.5% Triton X-100 (Wako Chemicals, Japan) in Dulbecco's Modified phosphate-buffered saline (D-PBS; GIBCO) for 30 min; and incubated with blocking solution containing 5% normal goat serum (NGS; Vector Laboratories, Burlingame, CA, USA), 5% normal donkey serum (NDS; Jackson ImmunoResearch, West Grove, PA, USA), 3% fetal bovine serum

(FBS; CCB, Japan) and 0.1% Tween 20 (Wako Chemicals, Japan) in D-PBS at 4°C overnight. Then, cells were incubated with primary antibodies, i.e., 2 µg/ml anti-OCT4 (Santa Cruz Biotechnology, Santa Cruz, CA, USA; C-10, SC-5279) and 20 µg/ml anti-SOX2 (Cell Signaling Technology, Danvers, MA, USA) in blocking buffer at 4 °C overnight. Following primary antibody incubation, cells were incubated with appropriate secondary antibodies -1.5 µg/ml DyLight 488 donkey anti-mouse IgG (Jackson ImmunoResearch) or 0.375 or 3 µg/ml DyLight 649 donkey anti-rabbit IgG (Jackson ImmunoResearch) in blocking buffer at room temperature for 1 h. Finally, cell nuclei were stained with 300 nM 4, 6-diamidino-2-phenylindole (DAPI; Dojindo, Japan) at room temperature for 30 min. Phase-contrast and fluorescent images of cells were recorded using inverted microscopy (Olympus IX71) equipped with a high-sensitive CCD camera (Olympus U-LH100HGAPO).

Flow cytometry: hiPSCs cultured on gelatin nanofiber, PDMS replica and PDMS replica²substrate were harvested with TrypLE Express. Cells were washed with PBS twice, and cell numbers were counted. For staining with antibodies, cells were diluted to a final concentration of 1×10^7 cells/ml in PBS with 2% FCS. Phycoerythrin (PE) anti-human SSEA4 or TRA-1-60 (Stemgent) labeled antibodies were added and incubated at room temperature for 30 min. As a negative control, specific isotype controls (PE Mouse IgG3 Isotype Control (Stemgent) and Dylight 488 mouse IgM Isotype Control (Stemgent)) were used. After removing antibodies by centrifugation at 1000 rpm for 5 min, cells were washed with PBS containing 2% FCS. Finally, cell suspensions were applied to a flow cytometry cell sorting (FACS) Canto II machine (BD Biosciences).

Total RNA purification: Total cellular RNA was harvested using the RNeasy Mini Kit (Qiagen, Valencia, CA) following the manufacturer's instructions. Total RNA concentrations were measured in a NanoDrop1000 machine (ThermoFisher, Japan).

Reverse transcription PCR (RT-PCR): Total RNA was reverse transcribed using the RT First Strand Kit (Qiagen) and the primer sets described in [16]. A reaction mixture (25 µl) containing 1 µl cDNA, 0.2µM PCR primers, and 5 units of Taq DNA polymerase (Takara, Japan) in PCR buffer was subjected to amplification in a DNA thermal cycler (Applied Biosystems 7300 Real-Time PCR System). PCR was performed for 30–35 cycles (94°C, 30 sec; 58°C, 30 sec; 72°C, 60 sec) with an initial incubation at 94°C for 5 min and a final extension at 68°C for 3 min. Amplified products (10 µl) were resolved by 1.2 % agarose gel electrophoresis and visualized by ethidium

bromide staining. RT-PCR results of glyceraldehyde-3-phosphate dehydrogenase were used for the control.

Scanning Electron Microscope (SEM) imaging: High-resolution images were taken with an SEM (JCM-5000; JEOL Ltd. Japan) operated at 10 kV. Prior to imaging, a 5-nm-thick gold layer was deposited on samples by sputtering (MSP 30T; Shinku Device, Japan).

3. Results

The fabrication process of gelatin nanofiber substrate has been optimized previously [16] and adopted in this work for the fabrication of nanocasting templates. Once fabricated, the surface pattern of the template was replicated into PDMS many times (**Fig. 1**). As can be seen in AFM images of the figure, the PDMS replica displays a complimentary surface morphology of the template. After gelatin coating, the contact angle of the replica (63.2°) is close to that of the gelatin nanofiber substrate (60.4°), both being hydrophilic and suited for cell seeding and cell attachment. In **Fig. S1**, the whole fabrication processes of PDMS replica and replica² before and after gelatin coating are shown. The surface roughness of the AFM images was analyzed by assuming a roughness profile of n orders. The arithmetic average of absolute values R_a and the root mean squared R_{rms} are calculated,

$$R_a = \frac{1}{n} \sum_{i=1}^n |y_i|, R_{rms} = \sqrt{\frac{1}{n} \sum_{i=1}^n y_i^2}$$

where y_i is the vertical distance from the mean line. As shown in **Fig. S1(c)**, R_a and R_{rms} of the PDMS replica were smaller than that of the gelatin nanofiber substrate (template), and that of the PDMS replica² were further reduced. In both cases, the roughness of the replicas decreases but the contact angle reduces after gelatin-coating. Fig. S2 scanning electron microscopy images of the gelatin nanofiber before and after crosslinking as well as photographs of 2 μ l water droplets on two types of replicas before and after gelatin deposition. As can be seen, the first-generation replica fairly reproduced the crosslinked nanofiber features but the second-generation degraded the nanofibers' morphology. This is often the case when PDMS is used as a template. Although the quality of the second-generation replica could be improved by using a template of harder material, this most mostly relied on the PDMS nanocasting for the sake of process simplicity. As can also be seen, the contact angles of the two types of replicas are comparable before and after gelatin

deposition, suggesting that they have comparable surface roughness though they are both smaller than that of the master.

After seeding, hiPSCs aggregated to form cell clusters in three hours and then cell colonies in one day, on both gelatin nanofiber substrate and PDMS replica, which is characteristic of the hiPSC expansion (**Fig. 2a, b**). hiPSCs were generated from somatic cells [44]. When just seeded, they had a round shape (Fig. 2a1, b1). On day 1, ROCK inhibitor (Y-27632) was applied and hiPSC colonies kept growing up to day 4 in E8 and E8flex media (**Fig. 2a2-4, 2b2-4**). Clearly, these hiPSC colonies were sharp-edged, flat, and ball-like monolayer structures termed "round colonies" (**Fig. 2a4, 2b4**), which is a typical undifferentiated ESC-like morphology [45]. No significant differences in the morphology of the cells and colonies could be observed during this period.

The morphologies of hiPSC colonies were also examined after passage. **Fig. 2c** and **2d** display the phase contrast images of the hiPSC colonies at passages 4, 6, 8, and 13, showing also comparable growth and formation of the hiPSC colonies. Here, the passages were performed at the same time for both types of substrates at 70-80% confluence, suggesting the same growth rate of the hiPSCs over a long period on both types of substrates. However, on PDMS replica² some cells appeared in the areas between colonies as marked by the red circles in **Fig. S3**, suggesting that cells underwent a spontaneous differentiation after three passages. **Fig. 3** shows alkaline phosphatase (AP) staining images of the hiPSCs on both types of the substrate at passage 5, confirming their undifferentiated state. In contrast, both AP staining and phase-contrast images of the hiPSCs on gelatin (without crosslinking) coated glass at passages 1 and 2 already showed a bad state of the cells (**Fig. S3**).

Immunocytochemistry analyses were performed with markers OCT4 and SOX2, which are essential transcription factors of pluripotent stem cells. As shown in **Fig. 4**, the two types of proteins were highly expressed in hiPSCs on both types of substrates at passage 9, also confirming maintained pluripotency of the hiPSCs cells. In contrast, on PDMS replica², the expression level of OCT4 became relatively low at passage 6, and some cells did not express OCT4 all as marked by small red cells in Fig S4.

Furthermore, flow cytometric analyses were performed using surface proteins, SSEA4 and TRA-1-60, of the hiPSCs at passage 9 (**Fig. 5**). As expected, both proteins were highly expressed

in the hiPSCs on both types of culture substrate, and quantitatively over 99.9% of the hiPSCs maintained their pluripotency. However, SSEA4 expression on the PDMS replica² substrate is comparatively lower with more than 0.2% cells without expression of neither SSEA4 nor TRA-1-60, suggesting them all in a completely differentiated state.

Finally, RT-PCR analyses were performed for hiPSCs on different types of substrates (**Fig. 6**). Clearly, the expression of pluripotency (OCT4, NANOG, and SOX2) and differentiation (PAX6, BRACHYURY, and AFP) genes of the hiPSCs on PDMS replica maintain similar levels of that on gelatin nanofiber substrates over 13 passages. However, the hiPSCs on PDMS replica² at passage 9 showed a high expression of BRACHYURY, indicating a significant deviation from the pluripotency state of the cells.

4. Discussions

Previously, we have reported a nanocasting method to replicate a lotus leaf with both micro and nano-scale features which are difficult to be created artificially [38]. Based on this approach, we fabricated templates with gelatin nanofibrous morphology. As can be seen in Fig. S2, the electrospun nanofibers after crosslinking showed multiple nanofiber cross-points and the morphology of the template could be fairly reproduced into PDMS. To make the PDMS replica suited for cell culture [46] and keep the consistency with our previous work, gelatin-coating was applied. As result, the gelatin-coated PDMS replica became hydrophilic with a contact angle comparable to that of the gelatin nanofiber substrate.

The mechanical properties and in particular the stiffness of the substrate play an important in the cell fate decision of the stem cells [19-32]. Stem cells probe the substrate and regulate the intracellular contractility and stiffness [17,25]. The pluripotency of the hiPSCs should be associated with their low contractility, suggesting the use of low stiffness substrate for long-term propagation of the substrate [25]. It has been recently shown that soft substrates (1.5 or 15 kPa PDMS) caused modulation of several cellular features into a phenotype closer to pluripotent stem cells due to increased expression of pluripotency-related genes [47]. In our case, the Young's modulus of the PDMS is in the order of 1 MPa [48]. The PDMS replica may have a smaller effective Young's modulus, due to nanofibrous surface morphology for the same reason as the micropillar deflection. Previously, an effective Young's modulus of PDMS pillars was much

smaller than that of a bulk PDMS [25, 26]. Although the nanofibrous morphology is significantly different from that of pillars, the bending effect of a featured structure with a lateral force exercised by cells should be qualitatively the same. Roughly speaking, an effective Young's modulus of ~ 211 kPa could be estimated by considering an array of pillars of $1\ \mu\text{m}$ diameter and $1\ \mu\text{m}$ height. On the other hand, Young's modulus of wetted gelatin is also in the order of 1 MPa [49,50]. By using the same technique described in [50], we measured the deflection of a bilayer structure, a monolayer of crosslinked gelatin on a thin PDMS layer, as a function of applied pressure. As result, an effective material Young's modulus in the order of 1 MPa was determined. According to the theory of cellular solids [51], the effective Young's modulus of a porous or structured material is always smaller than Young's modulus of the bulk material. For a suspended monolayer of crosslinked gelatin nanofibers, its in-plan effective Young's modulus can be as small as 1 kPa. When the monolayer is bonded with a PDMS layer, the stiffness should be different [52, 53] but in the same order of magnitude. In contrast, a nanofiber-covered glass substrate should have a much larger Young's modulus (>10 GPa) [54]. Finally, cells, and in particular the aggregated hiPSCs are generally not in conformal contact with a rough surface due to the surface tension of the cell membrane. This means that there is more free space for more efficient diffusion of nutrients and metabolites than that of the cells on a flat substrate. Therefore, the nanofibrous morphology is twice in favor of hiPSC culture and proliferation.

We would like to mention that although other types of biomolecules can be used to coat the surface of the PDMS replica, gelatin has been chosen for close comparison with gelatin nanofiber substrate. Furthermore, gelatin is low-cost and easy to process into thin films, nanofibers, microparticles, and encapsulations [55-58]. Depending on the crosslinking, the biodegradability of gelatin can be regulated. On the other hand, gelatin possesses the RGD sequences of collagen and the nanofibrous morphology of patterned gelatin promotes cell adhesion and cell proliferation. Matrigel is often used for hiPSC culture and self-renewing but it was produced from mouse cells with many unknown factors. Nevertheless, it is rich in ECM composition. Compared to Matrigel, gelatin is perhaps too pure. In this regard, new ECM components may be added and more systematic studies are expected.

5. Conclusions

We have developed a method to reproduce the nanofibrous morphology of a substrate by nanocasting with PDMS. This method is generic and low-cost. It can be easily implemented and scaled up for different applications. Our results showed that such a negative tone replica of the template could be used as a substrate for hiPSC propagation over tenth generations but the positive tone replica could not be used for long-term hiPSC propagation. The use of PDMS seems to be advantageous not only for easy casting not also for its relatively low stiffness often required in hiPSC differentiation. This method might find application cell-based assays or tissue engineering which are based on stringent considerations on material stiffness and surface morphology.

References

- [1] K. Takahashi, K. Tanabe, M. Ohnuki, M. Narita, T. Ichisaka, K. Tomoda, S. Yamanaka, Induction of pluripotent stem cells from adult human fibroblasts by defined factors, *cell* 131(5) (2007) 861-872.
- [2] I.-H. Park, N. Arora, H. Huo, N. Maherali, T. Ahfeldt, A. Shimamura, M.W. Lensch, C. Cowan, K. Hochedlinger, G.Q. Daley, Disease-specific induced pluripotent stem cells, *cell* 134(5) (2008) 877-886.
- [3] A. Sharma, S. Sances, M.J. Workman, C.N. Svendsen, Multi-lineage human iPSC-derived platforms for disease modeling and drug discovery, *Cell stem cell* 26(3) (2020) 309-329.
- [4] S.M. Wu, K. Hochedlinger, Harnessing the potential of induced pluripotent stem cells for regenerative medicine, *Nature cell biology* 13(5) (2011) 497-505.
- [5] U. Ahmed, R. Ahmed, M.S. Masoud, M. Tariq, U.A. Ashfaq, R. Augustine, A. Hasan, Stem cells based in vitro models: trends and prospects in biomaterials cytotoxicity studies, *Biomedical Materials* 16(4) (2021) 042003.
- [6] K. Ye, S. Jin, *Human embryonic and induced pluripotent stem cells: lineage-specific differentiation protocols*, Springer 2012.
- [7] N. Gunhanlar, G. Shpak, M. van der Kroeg, L. Gouty-Colomer, S. Munshi, B. Lendemeijer, M. Ghazvini, C. Dupont, W. Hoogendijk, J. Gribnau, A simplified protocol for differentiation of electrophysiologically mature neuronal networks from human induced pluripotent stem cells, *Molecular psychiatry* 23(5) (2018) 1336-1344.
- [8] C. Corrò, L. Novellademunt, V.S. Li, A brief history of organoids, *American Journal of Physiology-Cell Physiology* 319(1) (2020) C151-C165.
- [9] S.W. Chan, M. Rizwan, E.K. Yim, Emerging Methods for Enhancing Pluripotent Stem Cell Expansion, *Frontiers in Cell and Developmental Biology* 8 (2020) 70.
- [10] C.S. Hughes, L.M. Postovit, G.A. Lajoie, Matrigel: a complex protein mixture required for optimal growth of cell culture, *Proteomics* 10(9) (2010) 1886-1890.
- [11] S. Rodin, A. Domogatskaya, S. Ström, E.M. Hansson, K.R. Chien, J. Inzunza, O. Hovatta, K. Tryggvason, Long-term self-renewal of human pluripotent stem cells on human recombinant laminin-511, *Nature biotechnology* 28(6) (2010) 611-615.
- [12] T. Miyazaki, S. Futaki, K. Hasegawa, M. Kawasaki, N. Sanzen, M. Hayashi, E. Kawase, K. Sekiguchi, N. Nakatsuji, H. Suemori, Recombinant human laminin isoforms can support the undifferentiated growth of human embryonic stem cells, *Biochemical and biophysical research communications* 375(1) (2008) 27-32.

- [13] S.R. Braam, L. Zeinstra, S. Litjens, D. Ward - van Oostwaard, S. van den Brink, L. van Laake, F. Lebrin, P. Kats, R. Hochstenbach, R. Passier, Recombinant Vitronectin Is a Functionally Defined Substrate That Supports Human Embryonic Stem Cell Self - Renewal via $\alpha V\beta 5$ Integrin, *Stem cells* 26(9) (2008) 2257-2265.
- [14] L.G. Villa-Diaz, H. Nandivada, J. Ding, N.C. Nogueira-de-Souza, P.H. Krebsbach, K.S. O'Shea, J. Lahann, G.D. Smith, Synthetic polymer coatings for long-term growth of human embryonic stem cells, *Nature biotechnology* 28(6) (2010) 581-583.
- [15] Z. Melkounian, J.L. Weber, D.M. Weber, A.G. Fadeev, Y. Zhou, P. Dolley-Sonneville, J. Yang, L. Qiu, C.A. Priest, C. Shogbon, Synthetic peptide-acrylate surfaces for long-term self-renewal and cardiomyocyte differentiation of human embryonic stem cells, *Nature biotechnology* 28(6) (2010) 606-610.
- [16] L. Liu, M. Yoshioka, M. Nakajima, A. Ogasawara, J. Liu, K. Hasegawa, S. Li, J. Zou, N. Nakatsuji, K.-i. Kamei, Nanofibrous gelatin substrates for long-term expansion of human pluripotent stem cells, *Biomaterials* 35(24) (2014) 6259-6267.
- [17] R.I. Clyman, K.A. McDonald, R.H. Kramer, Integrin receptors on aortic smooth muscle cells mediate adhesion to fibronectin, laminin, and collagen, *Circulation research* 67(1) (1990) 175-186.
- [18] B. Joddar, C. Nishioka, E. Takahashi, Y. Ito, Chemically fixed autologous feeder cell-derived niche for human induced pluripotent stem cell culture, *Journal of Materials Chemistry B* 3(11) (2015) 2301-2307.
- [19] K. Saha, Y. Mei, C.M. Reisterer, N.K. Pyzocha, J. Yang, J. Muffat, M.C. Davies, M.R. Alexander, R. Langer, D.G. Anderson, Surface-engineered substrates for improved human pluripotent stem cell culture under fully defined conditions, *Proceedings of the National Academy of Sciences* 108(46) (2011) 18714-18719.
- [20] T.B. Bertucci, G. Dai, Biomaterial engineering for controlling pluripotent stem cell fate, *Stem cells international* 2018 (2018).
- [21] L.R. Cortella, I.A. Cestari, R.D. Lahuerta, M.C. Araña, M. Soldera, A. Rank, A.F. Lasagni, I.N. Cestari, Conditioning of hiPSC-derived cardiomyocytes using surface topography obtained with high throughput technology, *Biomedical Materials* 16(6) (2021) 065007.
- [22] E. Huethorst, M.F. Cutiongco, F.A. Campbell, A. Saeed, R. Love, P.M. Reynolds, M.J. Dalby, N. Gadegaard, Customizable, engineered substrates for rapid screening of cellular cues, *Biofabrication* 12(2) (2020) 025009.
- [23] Y. Li, L. Li, Z.-N. Chen, G. Gao, R. Yao, W. Sun, Engineering-derived approaches for iPSC preparation, expansion, differentiation and applications, *Biofabrication* 9(3) (2017) 032001.
- [24] S. Vignesh, A. Gopalakrishnan, M. Poorna, S.V. Nair, R. Jayakumar, U. Mony, Fabrication of micropatterned alginate-gelatin and k-carrageenan hydrogels of defined shapes using simple wax mould method as a platform for stem cell/induced Pluripotent Stem Cells (iPSC) culture, *International journal of biological macromolecules* 112 (2018) 737-744.
- [25] B. Wang, X. Tu, J. Wei, L. Wang, Y. Chen, Substrate elasticity dependent colony formation and cardiac differentiation of human induced pluripotent stem cells, *Biofabrication* 11(1) (2018) 015005.
- [26] B. Wang, J. Shi, J. Wei, X. Tu, Y. Chen, Fabrication of elastomer pillar arrays with elasticity gradient for cell migration, elongation and patterning, *Biofabrication* 11(4) (2019) 045003.
- [27] J. Li, F. Zhang, L. Yu, N. Fujimoto, M. Yoshioka, X. Li, J. Shi, H. Kotera, L. Liu, Y. Chen, Culture substrates made of elastomeric micro-tripod arrays for long-term expansion of human pluripotent stem cells, *Journal of Materials Chemistry B* 5(2) (2017) 236-244.
- [28] S. Ramakrishna, R. Jose, P. Archana, A. Nair, R. Balamurugan, J. Venugopal, W. Teo, *Science*

and engineering of electrospun nanofibers for advances in clean energy, water filtration, and regenerative medicine, *Journal of materials science* 45(23) (2010) 6283-6312.

[29] S.H. Lim, H.-Q. Mao, Electrospun scaffolds for stem cell engineering, *Advanced drug delivery reviews* 61(12) (2009) 1084-1096.

[30] H.F. Lu, K. Narayanan, S.-X. Lim, S. Gao, M.F. Leong, A.C. Wan, A 3D microfibrillar scaffold for long-term human pluripotent stem cell self-renewal under chemically defined conditions, *Biomaterials* 33(8) (2012) 2419-2430.

[31] T. Kaitsuka, R. Kojima, M. Kawabe, H. Noguchi, N. Shiraki, S. Kume, K. Tomizawa, A culture substratum with net-like polyamide fibers promotes the differentiation of mouse and human pluripotent stem cells to insulin-producing cells, *Biomedical Materials* 14(4) (2019) 045019.

[32] L. Wertheim, A. Shapira, R.J. Amir, T. Dvir, A microfluidic chip containing multiple 3D nanofibrillar scaffolds for culturing human pluripotent stem cells, *Nanotechnology* 29(13) (2018) 13LT01.

[33] D. Kumar, T.P. Dale, Y. Yang, N.R. Forsyth, Self-renewal of human embryonic stem cells on defined synthetic electrospun nanofibers, *Biomedical Materials* 10(6) (2015) 065017.

[34] W. Teo, S. Ramakrishna, Electrospun fibre bundle made of aligned nanofibres over two fixed points, *Nanotechnology* 16(9) (2005) 1878.

[35] L. Yu, J. Li, I. Minami, X. Qu, S. Miyagawa, N. Fujimoto, K. Hasegawa, Y. Chen, Y. Sawa, H. Kotera, Clonal Isolation of Human Pluripotent Stem Cells on Nanofibrillar Substrates Reveals an Advanced Subclone for Cardiomyocyte Differentiation, *Advanced healthcare materials* 8(13) (2019) 1900165.

[36] K.i. Kamei, Y. Mashimo, M. Yoshioka, Y. Tokunaga, C. Fockenber, S. Terada, Y. Koyama, M. Nakajima, T. Shibata - Seki, L. Liu, Microfluidic - Nanofiber Hybrid Array for Screening of Cellular Microenvironments, *Small* 13(18) (2017) 1603104.

[37] L. Liu, K.-i. Kamei, M. Yoshioka, M. Nakajima, J. Li, N. Fujimoto, S. Terada, Y. Tokunaga, Y. Koyama, H. Sato, Nano-on-micro fibrillar extracellular matrices for scalable expansion of human ES/iPS cells, *Biomaterials* 124 (2017) 47-54.

[38] M. Sun, C. Luo, L. Xu, H. Ji, Q. Ouyang, D. Yu, Y. Chen, Artificial lotus leaf by nanocasting, *Langmuir* 21(19) (2005) 8978-8981.

[39] Y. Chen, A. Pepin, Nanofabrication: Conventional and nonconventional methods, *Electrophoresis* 22(2) (2001) 187-207.

[40] C. Vieu, F. Carcenac, A. Pepin, Y. Chen, M. Mejias, A. Lebib, L. Manin-Ferlazzo, L. Couraud, H. Launois, Electron beam lithography: resolution limits and applications, *Applied surface science* 164(1-4) (2000) 111-117.

[41] S. Yadav, A. Majumder, Bio-mimicked hierarchical 2D and 3D structures from natural templates: applications in cell biology, *Biomedical Materials* (2021).

[42] T.E. Ludwig, V. Bergendahl, M.E. Levenstein, J. Yu, M.D. Probasco, J.A. Thomson, Feeder-independent culture of human embryonic stem cells, *Nature methods* 3(8) (2006) 637-646.

[43] K. Watanabe, M. Ueno, D. Kamiya, A. Nishiyama, M. Matsumura, T. Wataya, J.B. Takahashi, S. Nishikawa, S.-i. Nishikawa, K. Muguruma, A ROCK inhibitor permits survival of dissociated human embryonic stem cells, *Nature biotechnology* 25(6) (2007) 681-686.

[44] M. Patel, S. Yang, Advances in reprogramming somatic cells to induced pluripotent stem cells, *Stem Cell Reviews and Reports* 6(3) (2010) 367-380.

[45] L. Yu, J. Li, J. Hong, Y. Takashima, N. Fujimoto, M. Nakajima, A. Yamamoto, X. Dong, Y. Dang, Y. Hou, Low cell-matrix adhesion reveals two subtypes of human pluripotent stem cells, *Stem cell reports* 11(1) (2018) 142-156.

- [46] J.N. Lee, X. Jiang, D. Ryan, G.M. Whitesides, Compatibility of mammalian cells on surfaces of poly (dimethylsiloxane), *Langmuir* 20(26) (2004) 11684-11691.
- [47] H. Gerardo, A. Lima, J. Carvalho, J.R. Ramos, S. Couceiro, R.D. Travasso, R.P. das Neves, M. Grãos, Soft culture substrates favor stem-like cellular phenotype and facilitate reprogramming of human mesenchymal stem/stromal cells (hMSCs) through mechanotransduction, *Scientific reports* 9(1) (2019) 1-18.
- [48] M. Kim, B.-U. Moon, C.H. Hidrovo, Enhancement of the thermo-mechanical properties of PDMS molds for the hot embossing of PMMA microfluidic devices, *Journal of Micromechanics and Microengineering* 23(9) (2013) 095024.
- [49] S. Zhang, Y. Huang, X. Yang, F. Mei, Q. Ma, G. Chen, S. Ryu, X. Deng, Gelatin nanofibrous membrane fabricated by electrospinning of aqueous gelatin solution for guided tissue regeneration, *Journal of Biomedical Materials Research Part A: An Official Journal of The Society for Biomaterials, The Japanese Society for Biomaterials, and The Australian Society for Biomaterials and the Korean Society for Biomaterials* 90(3) (2009) 671-679.
- [50] M Radiom, Y He, J Peng-Wang, A Baeza-Squiban, JF Berret, Y Chen, *Biotechnology and Bioengineering*, 117 (2020): 2827– 2841
- [51] L.J. Gibson, Cellular solids, *Mrs Bulletin* 28(4) (2003) 270-274.
- [52] C. Luo, F. Meng, A. Francis, Fabrication and application of silicon-reinforced PDMS masters, *Microelectronics journal* 37(10) (2006) 1036-1046.
- [53] J. Shi, L. Liu, Y. Chen, Investigation of cell culture in microfluidic devices with different bi-layer substrates, *Microelectronic engineering* 88(8) (2011) 1693-1697.
- [54] S. Inaba, S. Fujino, K. Morinaga, Young's modulus and compositional parameters of oxide glasses, *Journal of the American Ceramic Society* 82(12) (1999) 3501-3507.
- [55] C.F. Guimarães, L. Gasperini, A.P. Marques, R.L. Reis, The stiffness of living tissues and its implications for tissue engineering, *Nature Reviews Materials* 5(5) (2020) 351-370.
- [56] S.-C. Wu, W.-H. Chang, G.-C. Dong, K.-Y. Chen, Y.-S. Chen, C.-H. Yao, Cell adhesion and proliferation enhancement by gelatin nanofiber scaffolds, *Journal of Bioactive and Compatible Polymers* 26(6) (2011) 565-577.
- [57] A.B. Bello, D. Kim, D. Kim, H. Park, S.-H. Lee, Engineering and functionalization of gelatin biomaterials: From cell culture to medical applications, *Tissue Engineering Part B: Reviews* 26(2) (2020) 164-180.
- [58] S. Li, J. Shi, L. Liu, J. Li, L. Jiang, C. Luo, K. Kamei, Y. Chen, Fabrication of gelatin nanopatterns for cell culture studies, *Microelectronic engineering* 110 (2013) 70-74.

Figure caption

Figure 1. Schematic presentation of the fabrication process of PDMS replica and AFM images of gelatin nanofiber substrate (left) and a PDMS replica (right). Inserts are photographs of 2 μ l water droplets deposited on the two types of substrates, showing a contact angle of 63.2° and 60.4° respectively.

Figure 2. Phase contract images of the hiPSCs on gelatin nanofiber substrate (a1-a4, c1-c4) and PDMS replica (b1-b4, d1-d4) after incubation for 3 h, 1, 2, and 4 days (a1-a4, b1-b4) and at passage 4, 6, 8, and 13 (c1-c4,d1-d4), respectively. Scale bar in (a1) and (b1) represents 50 μ m; scale bar in (a2-a4, b2-b4, c1-c4, d1-d4) represents 100 μ m.

Figure 3 Alkaline phosphatase (AP) staining images of the hiPSCs at passage 5 on gelatin nanofiber substrate (a1-a3) and PDMS replica (b1-b3), respectively. The diameter of the culture dish in (a1) and (b1) is 35mm. Scale bar in (a2) and (b2) represents 200 μ m, scale bar (a3) and (b3) represents 100 μ m.

Figure 4. Immunocytochemical images of OCT4 (green) and SOX2 (red) marked hiPSCs at passage 9 on gelatin nanofiber substrate (a1-a3) and PDMS replica, respectively. Cell nuclei stained with DAPI (blue). Scale bar represents 100 μ m.

Figure 5. Flow cytometric results of SSEA4 and TRA-1-60 expression level of the hiPSCs on different types of substrates including gelatin nanofiber substrate, PDMS replica (negative tone), and PDMS replica² (positive tone) at passage 9.

Figure 6. RT-PCR results of the hiPSCs on gelatin nanofiber substrate and PDMS replica at passage 13 on PDMS replica² at passage 8, respectively.

Figure 1

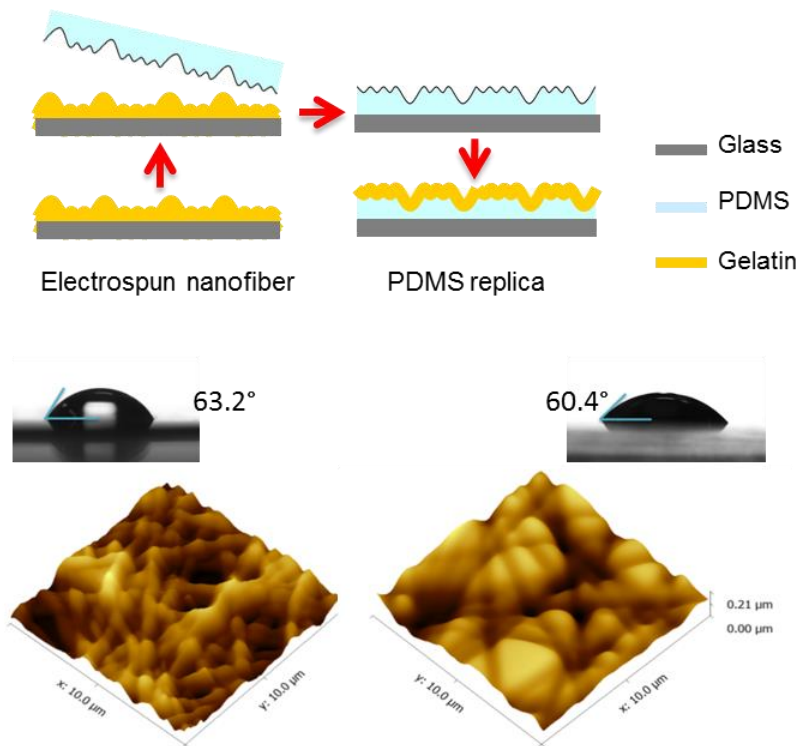


Figure 2

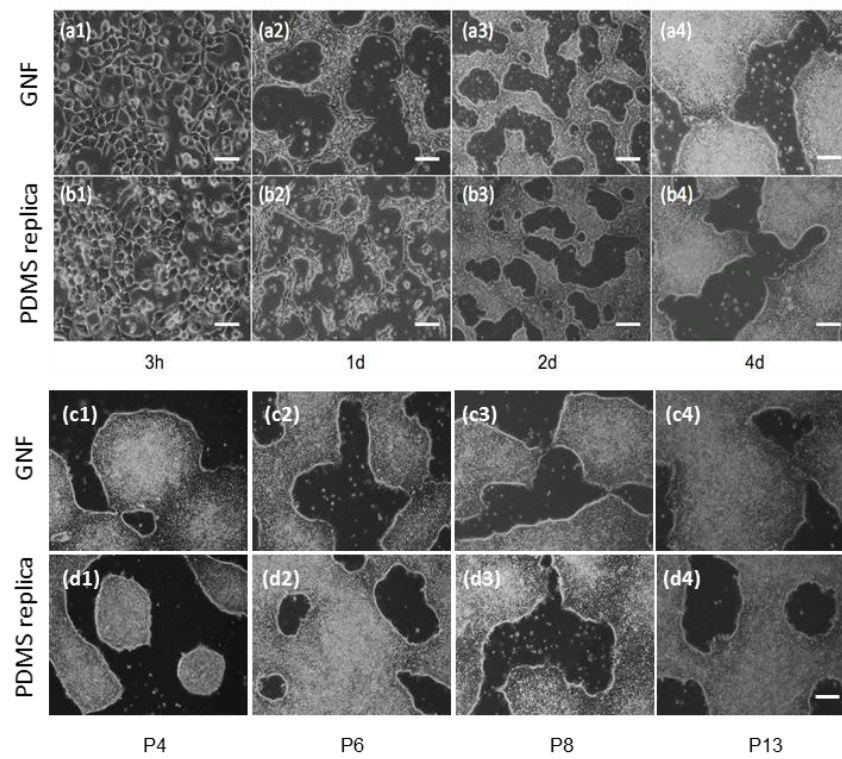


Figure 3

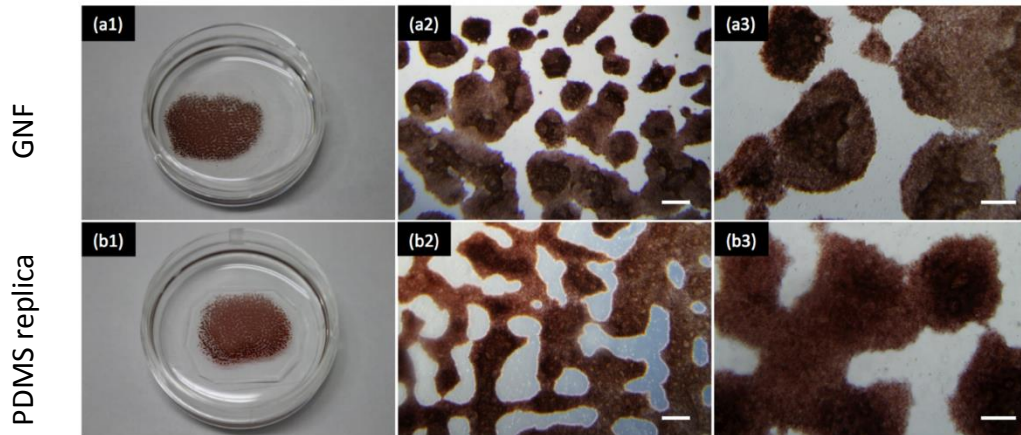


Figure 4

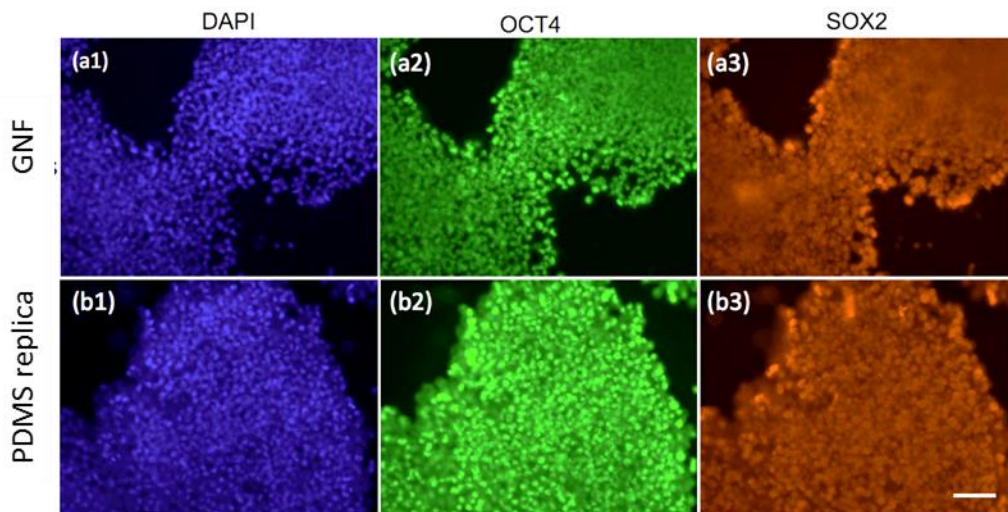


Figure 5

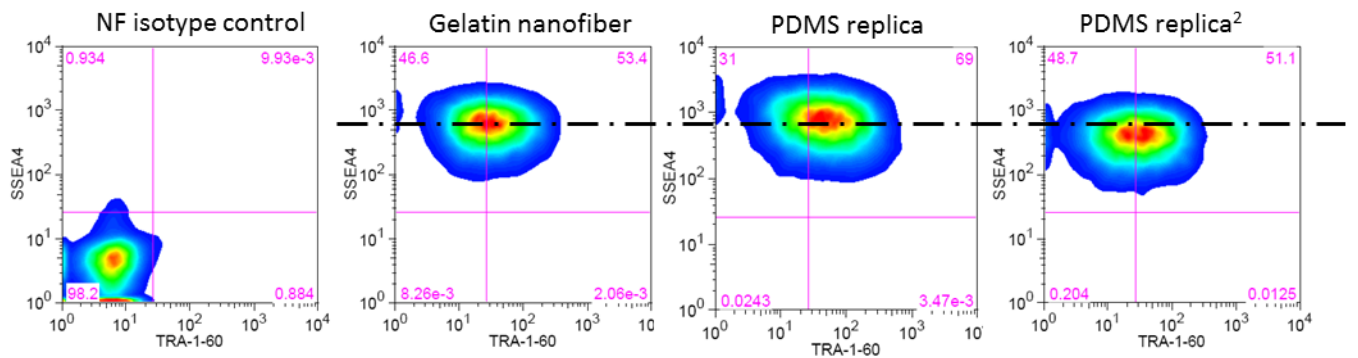


Figure 6

